John Paul Adrian Glaubitz

Doctoral Thesis Research Proposal

Department of Physics

Faculty of Mathematics and Natural Sciences

University of Oslo

Provisional Thesis Title

Nanostructuring of Si and ZnO by ion irradiation; electrical characterization

Names of Supervisors

- Prof. Dr. Bengt Gunnar Svensson
- Dr. Lasse Vines

This report will describe the project proposal for the research program that will lead John Paul Adrian Glaubitz to the Ph.D. degree at the University of Oslo, including scope, methodology and work plan. The main work will be carried out in the LENS group at Department of Physics/SMN, under supervision of Professor Bengt G. Svensson and Dr. Lasse Vines. The synthesis and characterization will mainly be carried out at the Micro- and Nanolaboratory (MiNaLab) at UiO.

1 Introduction

When the bi-polar junction transistor first saw the light of the day at Bell Laboratories in 1947, it did not only render the vacuum tube obsolete in most applications nearly over night but also created the whole new industry branch of semiconductor components. For most semiconductor devices, silicon is the preferred basis material which has to undergo several process steps during manufacturing until the desired electrical properties of the material are achieved. Certainly, the most fundamental and important of all process steps is the doping which dramatically changes the electrical conductivity of the semiconductor material by introducing impurities into the crystal which provide additional negative (donor impurities) or positive carriers (acceptor impurities). These impurities can either be introduced by thermal diffusion, a process in which the semiconductor material is immersed into an atmosphere of vaporized doping atoms within a furnace, or by ion implantation where the doping atoms are directly implanted into the semiconductor in the form of energetic ions. The big advantage of ion implantation over classical diffusion is that the doping of the target material can be very accurately controlled by tuning the proper ion energy and by blocking the ion beam from irradiating certain parts of the target. Thus, very thin doping regions as well as complex patterns of doping of the material can be achieved.

However, the penetration of the ions into the lattice does not only introduce the desired impurities (dopants) into the crystal but also defects, that is, abnormalities in the periodicity of the lattice which can dramatically influence the devices performance. These defects are therefore an important matter of research within the field of semiconductor physics. Numerous fundamental questions are yet to be answered and some of them shall be the subject of this research.

2 Scope of the proposed research

The overall objective is to investigate the electrical properties of nanometer-sized structures in Si and ZnO. In particular, embedded defect structures after irradiation by swift ions will be studied, including the evolution of the defect clusters during post-irradiation heat treatment (annealing). Defect clusters of this type are considered as potential candidates to enhance low energy photon absorption in future generation solar cells and hence increase the cell efficiency. The investigations are primarily of fundamental character, and a natural starting point for the thesis work will be the studies conducted previously by Vines et al. [1, 2, 3, 4]. The topic will be approach experimentally from both a macroscopic and microscopic point of view. For example, deep level transient spectroscopy (DLTS) is a powerful macroscopic technique for probing point defects in semiconductors, and can give valuable information about the band gap position and capture cross sections of the defect structures. On the other hand, scanning probe microscopy related techniques like scanning capacitance microscopy (SCM) and scanning spreading resistance microscopy (SSRM) will be utilized to extract both dimensional and electrical information on the nanometer scale. Here, it must be mentioned that a new SPM instrument with electrical characterization and variable temperature capabilities will be installed in MiNaLab during the spring 2011. Combining electrical characterization with a variable temperature makes the instrument unique and part of this Ph.D. project will concern developing and exploring these capabilities. For example, varying the temperature during nano-scale capacitance or resistance measurements bridges the gap between spectroscopic techniques like DLTS and nano-scale microscopy techniques, and thus, an ideal tool for probing ion-induced nanostructures in Si and ZnO.

3 Methodology

Here I will introduce the primary experimental tools and techniques which will be employed in the studies. These include various established spectroscopic as well as microscopic measurement techniques as well as the use of computer aided simulations. The methods are shortly described as well as their specific application in the research.

3.1 DLTS: Deep-level transient spectroscopy

Deep-level transient spectroscopy or short, DLTS, is a spectroscopic method to characterize traps, that is donor and acceptor levels, in semiconductors. It was first described by D.V. Lang in 1974 at Bell Labs [5]. DLTS measures the transient capacitance of a p-n junction or Schottky contact after injecting minority or majority carriers into the depletion region of the junction/contact. The injection occurs through an external RF pulse generator which generates short changes in junction bias either by applying a short forward pulse (injection of minority carriers) or by momentarily reducing the reverse bias (to inject majority carriers). Excess injected carriers are trapped in defect energy levels which lie in-between the conduction and valence bands in the depletion region. The trapped carriers are captured (during injection) and emitted (during relaxation of the system into equilibrium) with capture and emission rates characteristic to the appropriate energy levels of the defects. By performing these measurements at different temperatures, it is possible to obtain a temperature-dependent spectrum of the trap concentration. The reason is that by varying the temperature, one can tune the effective Fermi level and thus set an emission rate window in which only traps within that window contribute to the DLTS signal. On the resulting spectrum, each trap is represented by a peak whose sign determines whether it is a minority or majority carrier trap while the height of the peak determines the trap concentration. Figure 1 shows a typical DLTS spectrum from [6].

DLTS will be one of our main tools to examine defect levels and traps introduced by ion implantation. The current setup allows to sweep the sample temperature over a wide range thus allowing for probing in a wide spectrum of defect levels. The disadvantage of DLTS is that it is not possible to localize the defects within the bulk, all defects within the depletion region account for the concentration at a certain defect energy level, thus the term *defect concentration*. This deficiency can, however, be overcome when using methods based on the *scanning probed microscopy* to probe for the defect levels and carrier concentrations. Both *scanning capacitance microscopy* as well as *scanning spreading resistance microscopy*

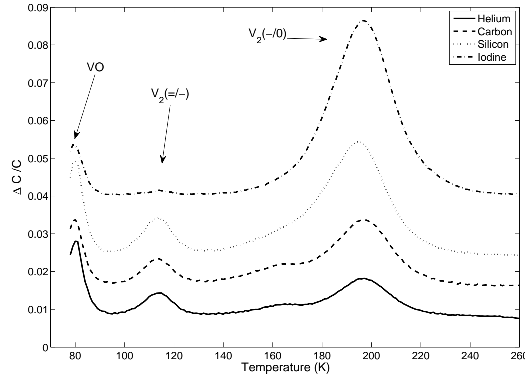

Figure 1: DLTS spectra of epitaxial Si after implantation with different ions (from [4]).

are enhancements of one the of classical SPM methods, namely *atomic force microscopy* (AFM) which is briefly introduced in the next section.

3.2 AFM: Atomic force microscopy

Unlike all imaging methods employing the diffraction of electron and light beams at crystal lattices, atomic force microscopy (AFM, sometimes also referred to as "scanning force microscopy") provides a means to resolve local structures and defects since it provides a direct microscopic image of the topography of a surface of a macroscopic object. AFM was developed in 1986 by Gerd Binnig et al. [7] as a consequent variant of its precursor, the scanning (electron) tunneling microscope [8] whose greatest disadvantages are the requirements of a conducting sample surface as well as relatively stable measurement conditions [1]. While the latter maps the topography of the surface by scanning along the lateral directions while measuring a vacuum tunneling current between the probe tip and the conductive sample surface, AFM measures the deflection of a small cantilever with a small tip due to the inter-atomic forces between tip and surfaces atoms. The deflection of the cantilever is detected over the reflection of a laser beam from the backside of the cantilever into an array of photo diodes (Fig. 2. Not only does AFM provide a means to probe non-conductive materials but it also allows to conduct easy measurements under ambient pressure and on liquids. The latter is performed with the AFM set to *tapping mode*, in which the cantilever is driven into oscillation by an external source. The other two principal modes being *contact mode* and *non-contact mode* with and without touching the surface to be probed respectively. While contact mode allows to work with rigid samples covered by soft adsorbates by being able to penetrate the soft layer, for example, non-contact mode has the advantage that the tip won't "snap-in" to the surface which can degrade the tip very quickly. However, non-contact mode requires very small distances to the surface while the surface has to be clean otherwise the results might be vary[2].

Tapping mode combines the advantages of *contact* and *non-contact mode* by dynamically touching the surface. This reduces the damage of tip and surface to a minimum while still being able to penetrate soft adsorbates. The gentle tapping also allows for probing of soft and liquid surfaces which is often dealt with when measuring under ambient conditions.

As mentioned before, we will use two special variants of AFM, one is the so-called *scanning capacitance microscopy* and the other one *scanning spreading resistance microscopy* which both measure electrical parameter while probing the surface.

[1]STM measurements are therefore usually conducted in ultra-high vacuum

[2]In non-contact mode, a thin albeit soft layer on the sample surface can dramatically impact the imaging results as the tip is unable to penetrate this layer to probe the actual sample surface

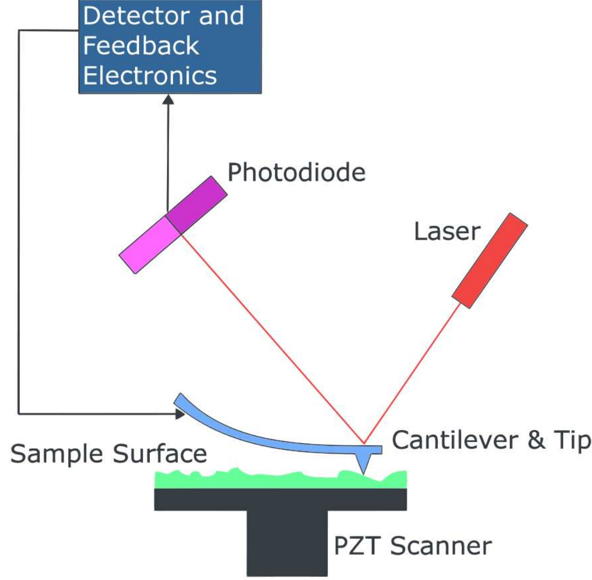

Figure 2: Schematical view of principal AFM operation (Source: Wikipedia).

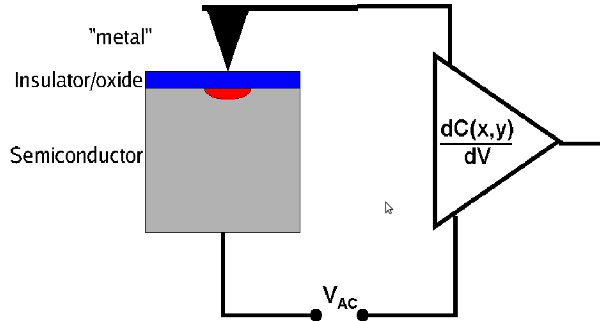

Figure 3: Schematical view of principal SCM operation (from: [1]).

3.3 SCM: Scanning capacitance microscopy

Using an electrically active AFM tip allows measurements of the capacitance and electrical resistance between surface and tip. These measurements form the basis of *scanning capacitance microscopy* [9, 10] and *scanning spreading resistance microscopy* [11]. Naturally, for SCM the AFM is operated in contact mode and probe tip, sample and readout unit form an electrical circuit (Fig. 3). The capacitance is determined by the capacitance of semiconductor C_{semi} and its oxide layer C_{ox}, the total capacitance is therefore easily obtained through:

$$\frac{1}{C_{tot}} = \frac{1}{C_{ox}} + \frac{1}{C_{semi}} \tag{1}$$

Thus the total capacitance can be considered as a series combination of oxide and semiconductor capacitance.

To calculate both C_{ox} and C_{semi}, we assume that there are no free carriers in the bulk of oxide and semiconductor and carrier neutrality outside of it (*depletion approximation*) and model the capacitances as plate capacitors, thus:

$$C_{ox} = \frac{A_{tip}\epsilon_{ox}}{d_{ox}} \tag{2}$$

with A_{tip} being the effective tip area size, ϵ_{ox} the permittivity and d_{ox} the thickness of the oxide layer.

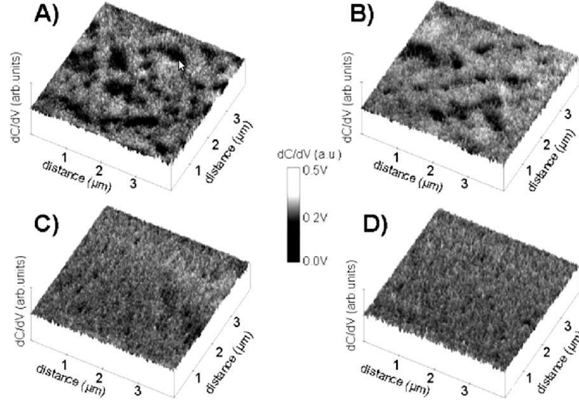

Figure 4: SCM images of Si samples implanted with 3 MeV Au^{2+} ions with dose $5 \times 10^{9}\text{cm}^{-2}$ (A), $8 \times 10^{8}\text{cm}^{-2}$ (B) and $2 \times 10^{8}\text{cm}^{-2}$ (C), as well as a implanted sample (D) (from [2]). These images show dose-dependent changes in the electronic structure of the Si bulk which are not visible in the topography scans of the AFM (Fig. 5).

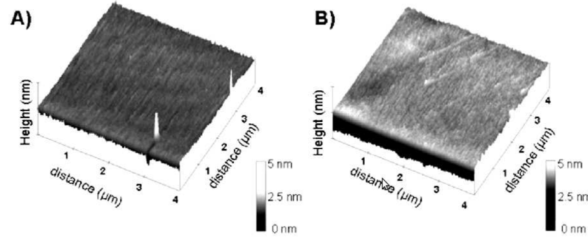

Figure 5: Topography scan (A) of the Si sample implanted with 3 MeV Au^{2+} ions with dose $5 \times 10^{9}\text{cm}^{-2}$ from Fig. 4 compared with a reference sample (B); there are no visible changes in the topography of the scan in (A) after ion bombardment. The electronic changes are only visible in the SCM images (Fig. 4).

For the semiconductor, the thickness of depletion region and thus the effective plate distance d_{semi} depend on the doping N_d and the contact potential V_0, as well as the applied bias V, thus:

$$C_{semi} = \frac{A_{tip}\epsilon_{semi}}{\sqrt{\frac{2\epsilon_{semi}(V_0 - V)}{qN_d}}} \tag{3}$$

and for the total capacitance:

$$C_{tot} = \frac{A_{tip}}{\sqrt{\frac{2(V_0 - V)}{\epsilon_{semi} q N_d}} + \frac{d_{ox}}{\epsilon_{ox}}} \tag{4}$$

Since A_{tip} is very small, the measured capacitances are usually very small (on the order of 10^{-18}F) and therefore neglectable compared stray capacitances of the measurement setup. It is therefore more reasonable to measure the changes in capacitance, thus $\frac{dC}{dV}$ with a typical lock-in amplifier setup. As mentioned before, SCM allows to visualize changes on the electronic scale which are not visible with AFM, compare Fig. 4 and 5. While the topography of the surface remains unchanged as can be seen from the AFM images, electrically active defects have been produced by the ion irradiation and can readily be seen in the SCM images. More recent developments in SCM provide higher resolutions [12] and even allow to perform measurements on doping profiles smaller than the diameter of the probe tip [13]. SCM also finds application in studying quantum wells [14, 15].

3.4 SSRM: Scanning spreading resistance microscopy

With SSRM [11] we determine the carrier concentration in the probed area by measuring the local spreading resistance in a contact-type AFM measurement. The spreading resistance R_s is related to the resistivity ρ which is proportional to the conductivity σ of the sample which depends on the carrier concentration:

$$R_s = \frac{\rho}{A_{tip}} \tag{5}$$

$$\frac{1}{\rho} = \sigma = q(n\mu_n + p\mu_p) \tag{6}$$

where R_s are the spreading resistance, A_{tip} the effective contact size[3] through the probing tip, q the elemental charge, n and p the negative and positive carrier concentrations respectively together with their mobilities μ_n and μ_p. In order to reduce the contact resistance, high contact forces are required which may lead to a fast deterioration of the probe tip. Another problem is that it is very difficult to determine the tip size and to maintain it over several measurements due to deodorization or changing of the tip. It is therefore very often desired to calibrate the SSRM setup before measurements.

Performing the SSRM measurements in a ultra-high vacuum (UHV) has been proven to drastically improve the resolution and the signal to noise ratio [17].

The total resistance of the typical SSRM measurement setup is constituted of:

$$R_{tot} = R_s + R_c + R_{tip} + R_{bulk} \tag{7}$$

While R_S denotes the spreading resistance, R_c, R_{tip} and R_{bulk} account for the contact, tip and bulk resistance. The latter incorporates the resistance of the lattice bulk, the back contact, wiring and the readout unit. Thus, if the other contributions are kept sufficiently low, R_{tot} is inversely proportional to the carrier concentration:

$$R_{tot} = \frac{1}{q(n\mu_n + p\mu_p)} \tag{8}$$

3.5 SRIM: Simulation of stopping and range of ions in matter

Besides the experimental techniques mentioned so far, we also rely on theoretical calculations to examine the defects introduced by heavy ion irradiation. The preferred simulation software for this matter is **SRIM** which abbreviates from *Simulation of stopping and range of ions in matter.* The software was developed Ziegler et al [16] and first published 1985. SRIM features around 28,000 built-in experimental data for stopping power and therefore allows for accurate simulation of ion penetration into matter. The stopping power is an essential parameter when ions penetrate matter. It defines how much energy per unit path length an ion loses when penetrating a crystal, thus the stopping power is usually measured in units of eVcm^{-1}. The stopping power depends primarily on the type of material which is penetrated and on the ion energy, Fig. 6 shows two typical plots where the author has performed a stopping power simulation using SRIM-2008.04 for both Hydrogen and Gold ions shot onto a Silicon target.

It can also create three-dimensional plots of the ion distribution when penetrating matter, including the trace of defects created by the ion beam and its so-called straggle and all resulting cascades which can occur when atoms are kicked out of their lattice position, becoming an interstitial atom which can subsequently hit other lattice atoms. Such a plot is shown in Fig. 7, (A).

Furthermore, one can calculate vacancy distributions (Fig. 7, (B) and (C)), sputtering rates, phonon production and ionization.

4 Schedule/Timeline of Research

A preliminary time schedule of the project is listed including an outline of the work which will be emphasized.

[3]For a cylindrical contact, $A_{tip} = 4 \times r_{cyl}$ and, for a hemisphere shape probe tip, $A_{tip} = 2\pi \times r_{hem}$ with r_x being the radii associated with a cylinder and hemisphere volume respectively. A typical tip radius is around $10 - 40$nm.

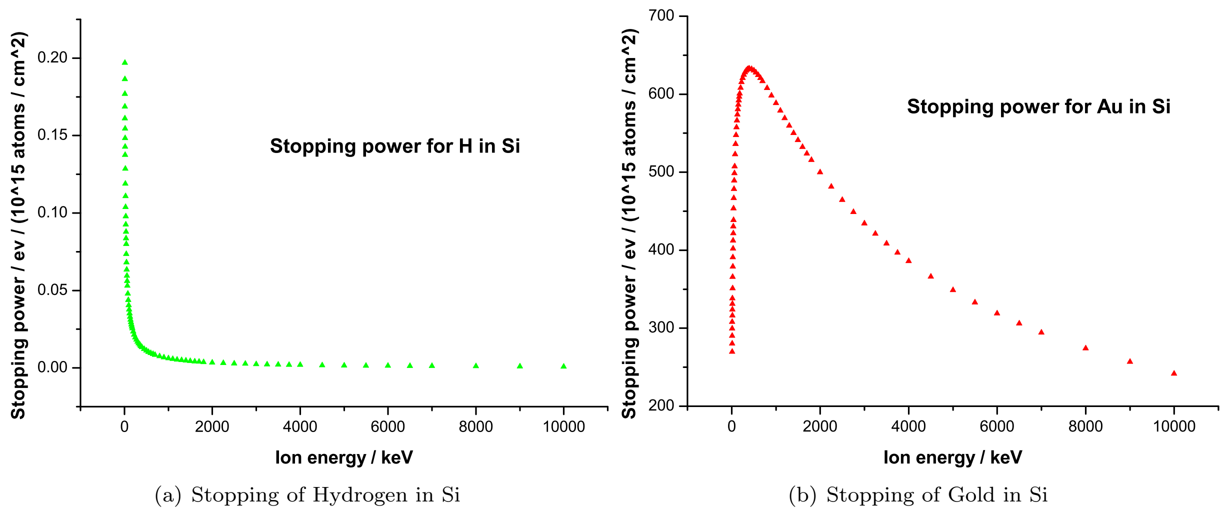

(a) Stopping of Hydrogen in Si

(b) Stopping of Gold in Si

Figure 6: SRIM simulations for stopping powers of H and Au in Si. The plots show the nuclear stopping of Hydrogen (a) and Gold (b) respectively in Silicon (100% mass composition). The units for the stopping were chosen to be $\mathrm{eV}/(1 \times 10^{15}\mathrm{atoms}/\mathrm{cm}^2)$. The plots indicate that there is a much stronger ion energy correlation for the stopping power for the heavy Au ions (196 amu) than for the light H ion (1 amu).

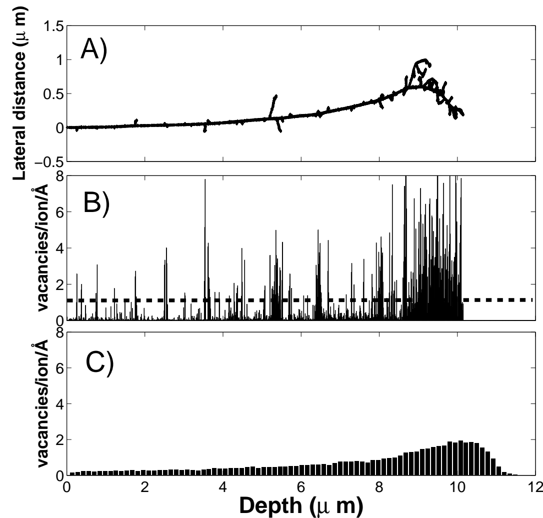

Figure 7: SRIM simulation of 46 MeV ion impact in Si, generating ion tracks (A) and a vacancy distribution (B); (C) shows the average vacancy distribution after 400 impacts (from: [4]).

4.1 Autumn 2010

- literature study of project related topics
- introduction to experimental techniques relevant for the Ph.D. project
- experimental training using available samples
- design of experiment and preparation of samples

4.2 Spring 2011

- course: FYS9310 - Material science of semiconductors
- course: MNSES9100 - Science, Ethics and Society
- compulsary teaching/tutoring
- investigation of ion-induced nano-channels in n-type Si (with variable doping concentration) using DLTS
- investigating diffusion of the nano-channels after thermal treatments using room temperature SPM
- start developing the variable temperature SPM
- data evaluation and simulation
- participate at the 24th *Nordic Semiconductor Meeting* in Aarhus, Denmark

4.3 Autumn 2011

- course: FYS9430 - Condensed Matter Physics II
- compulsory teaching/tutoring
- investigation of ion-induced nano-channels in n-type ZnO
- continue investigation of ion-induced nano-channels in n-type Si (with variable doping concentration) using DLTS
- continue investigating of diffusion of the nano-channels after thermal treatments using room temperature SPM
- data evaluation and simulation
- start writing a paper on ion induced nano-channels in n-type Si
- continue developing the variable temperature SPM

4.4 Spring 2012

- course: UNIK9310 - Electron structure in Semiconductors
- compulsory teaching/tutoring
- characterize ion-induced nano-channels in Si using the variable temperature SPM
- characterize ion-induced nano-channels in ZnO using the variable temperature SPM
- parallel investigation of ion-induced nano-channels with DLTS
- data evaluation and simulation
- attend one international conference
- submit one regular journal paper

4.5 Autumn 2012

- compulsory teaching/tutoring
- continue characterization of ion-induced nano-channels in Si using the variable temperature SPM
- continue characterization of ion-induced nano-channels in ZnO using the variable temperature SPM
- parallel investigation of ion-induced nano-channels with DLTS
- data evaluation and simulation
- begin to sum up previous results in one or two more papers

4.6 Spring 2013

- compulsory teaching/tutoring
- continue characterization of ion-induced nano-channels in Si using the variable temperature SPM
- continue characterization of ion-induced nano-channels in ZnO using the variable temperature SPM
- parallel investigation of ion-induced nano-channels with DLTS
- data evaluation and simulation
- attend one international conference (EMRS for example)
- submit two regular journal papers

4.7 Autumn 2013

- compulsory teaching/tutoring
- continue characterization of ion-induced nano-channels in Si using the variable temperature SPM
- continue characterization of ion-induced nano-channels in ZnO using the variable temperature SPM
- parallel investigation of ion-induced nano-channels with DLTS
- data evaluation and simulation
- write and submit one regular journal paper

4.8 Spring 2014

- begin to write thesis
- compulsory teaching/tutoring
- data evaluation and simulation

4.9 Autumn 2014

- finish thesis and submission
- compulsory teaching/tutoring

References

[1] Lasse Vines. *Fundamental Defect Complexes and Nanostructuring of Silicon by Ion Beams.* PhD thesis, The University of Oslo, Oslo, 2008.

[2] Lasse Vines, Edouard Monakhov, Bengt G. Svensson, Jens Jensen, Anders Hallén, and Andrej Yu. Kuznetsov. Visualization of MeV ion impacts in Si using scanning capacitance microscopy. *Phys. Rev. B*, 73(8):085312–, February 2006.

[3] L. Vines, E. Monakhov, K. Maknys, B.G. Svensson, J. Jensen, A. Hallén, and A. Yu. Kuznetsov. Scanning probe microscopy of single Au ion implants in Si. *Materials Science and Engineering: C*, 26(5-7):782–787, July 2006.

[4] L. Vines, E. V. Monakhov, J. Jensen, A. Yu. Kuznetsov, and B. G. Svensson. Effect of spatial defect distribution on the electrical behavior of prominent vacancy point defects in swift-ion implanted si. *Phys. Rev. B*, 79(7):075206–, February 2009.

[5] D. V. Lang. Deep-level transient spectroscopy: A new method to characterize traps in semiconductors. *J. Appl. Phys.*, 45(7):3023–3032, July 1974.

[6] R. Langfeld. A new method of analysis of dlts-spectra. *Applied Physics A: Materials Science & Processing*, 44(2):107–110, 1987-10-01.

[7] G. Binnig, C. F. Quate, and Ch. Gerber. Atomic force microscope. *Phys. Rev. Lett.*, 56(9):930–, March 1986.

[8] G. Binnig, H. Rohrer, Ch. Gerber, and E. Weibel. Surface studies by scanning tunneling microscopy. *Phys. Rev. Lett.*, 49(1):57–, July 1982.

[9] W.P. Hough C.C. Williams, J. Slinkman and H.K. Wickramasinghe. Lateral dopant profiling with 200 nm resolution by scanning capacitance microscopy. *Appl. Phys. Lett.*, 55:1662, 1989.

[10] C. C. Williams. Two-dimensional dopant profiling by scanning capacitance microscopy. *Annual Review of Materials Science*, 29:471–504, 1999.

[11] P. De Wolf, J. Snauwaert, T. Clarysse, W. Vandervorst, and L. Hellemans. Characterization of a point-contact on silicon using force microscopy-supported resistance measurements. *Appl. Phys. Lett.*, 66(12):1530–1532, March 1995.

[12] Filippo Giannazzo, Francesco Priolo, Vito Raineri, and Vittorio Privitera. High-resolution scanning capacitance microscopy of silicon devices by surface beveling. *Appl. Phys. Lett.*, 76(18):2565–2567, May 2000.

[13] F. Giannazzo, D. Goghero, V. Raineri, S. Mirabella, and F. Priolo. Scanning capacitance microscopy on ultranarrow doping profiles in si. *Appl. Phys. Lett.*, 83(13):2659–2661, September 2003.

[14] F. Giannazzo, V. Raineri, A. La Magna, S. Mirabella, G. Impellizzeri, A. M. Piro, F. Priolo, E. Napolitani, and S. F. Liotta. Carrier distribution in quantum nanostructures by scanning capacitance microscopy. *J. Appl. Phys.*, 97(1):014302–7, January 2005.

[15] F. Giannazzo, V. Raineri, S. Mirabella, G. Impellizzeri, and F Priolo. Drift mobility in quantum nanostructures by scanning probe microscopy. *Appl. Phys. Lett.*, 88(4):043117–3, January 2006.

[16] James F. Ziegler, M.D. Ziegler, and J.P. Biersack. SRIM - the stopping and range of ions in matter (2010). *Nuclear Instruments and Methods in Physics Research Section B: Beam Interactions with Materials and Atoms*, 268(11-12):1818–1823, June 2010.

[17] P. Eyben, S.-C. Vemula, T. Noda, and W. Vandervorst. Two-dimensional carrier profiling with sub-nm resolution using ssrm: From basic concept to tcad calibration and device tuning. In *Junction Technology, 2009. IWJT 2009. International Workshop on DOI - 10.1109/IWJT.2009.5166223*, pages 74–78, 2009.

5 Signatures

Date and signature, principal supervisor

Date and signature, subsidiary supervisor

Date and signature, Ph.D. candidate